PHYSICAL REVIEW A VOLUME 17, NUMBER 4 APRIL 1978

Picosecond relaxation measurements by polarization spectroscopy in condensed phases

J. J. Song, J. H. Lee, and M. D. Levenson
University of Southern California, University Park, Los Angeles, California 90007
(Received 25 October 1977)

A frequency domain technique is demonstrated which permits the determination of the homogeneous linewidth and relaxation rates of inhomogeneously broadened transitions in crystals, liquids, and glasses. The density-matrix formalism is employed to explain the origins of the intensity-dependent dichroism and birefringence observed in these experiments and to extract the relevant relaxation times. The samples initially studied were liquid solutions of the organic dyes malachite green and 1,3'-diethyl-2,2' quinolylthiacarbocyanine iodide. The ground-state recovery times were found to be 1.2 ± 0.1 and 3.4 ± 0.4 ps, respectively, for the two dyes in water solution. The transverse relaxation times were estimated to be less than 0.02 ps. The present technique is compared to resonant Rayleigh-type three-wave mixing and to time-resolved spectroscopic techniques.

I. INTRODUCTION

Many techniques of laser spectroscopy have been developed to resolve fine structures in the absorption and emission spectra of vapors.[1] The overall width of such a line often results from inhomogeneous broadening due to the random distribution of thermal velocities rather than from the linewidth of the transition of the individual atoms or molecules. In these cases the homogeneous linewidth of the transition can be measured by techniques in which a certain class of molecules within the velocity distribution selectively interacts with the laser light.[2]

In crystals, glasses, and liquids many transitions are inhomogeneously broadened by the random distribution of local strains at the sites of the absorbing centers. Some of these systems have been studied by the technique of laser-induced fluorescence line narrowing and by using coherent optical transients.[3,4] Nonfluorescing systems with short relaxation times have proved more difficult; some relaxation parameters have, however, been estimated using picosecond lasers or three-wave-mixing spectroscopy.[5,6]

We report here a technique in which the dichroism and birefringence induced in an absorbing sample by one laser field is detected by another. Our technique is similar to the polarization spectroscopy of Hänsch, Wieman, and Teets and is related to the Rayleigh resonance work of Yajima in the same way that our previous Raman-induced Kerr effect technique (RIKES) is related to coherent anti-Stokes Raman spectroscopy (CARS).[6,7] As in the case of RIKES the present technique is easier to execute experimentally and the results are more readily interpreted.

The overall scheme of the experiment is diagrammed in Fig. 1. A linearly, circularly, or elliptically polarized pumping wave at frequency ω_1 is incident upon an absorbing sample. The pumping wave creates an intensity and frequency-dependent birefringe and dichroism which is probed by a second wave at frequency ω_2. Generally this probe wave is linearly polarized at 45° to the major axis of the elliptically polarized pump. The nonlinear interaction produces a polarization component at the probe frequency that is orthogonal to the initial probe polarization. This new polarization component can then be detected in a variety of ways and its intensity plotted as a function of the difference in laser frequencies. Note that in contrast to the three-wave-mixing technique, there is no wave-vector matching condition.[6]

The dielectric polarization giving rise to this new polarization component can be found by solving the equations of motion for the density matrix describing the absorbing system. The resulting electric field and optical intensity can be obtained by integrating Maxwell's wave equation in the slowly varying amplitude and phase approximation.

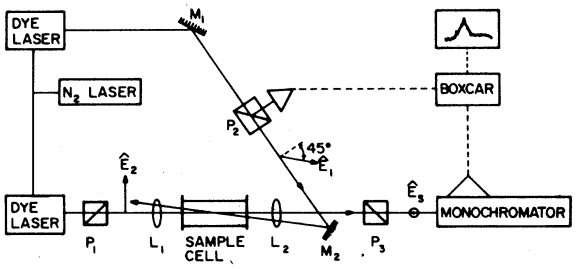

FIG. 1. Experimental setup. P, L, and M are the polarizer, lens, and mirror, respectively. The dye laser beam which goes through the crossed polarizers p_1 and p_3 is the probe beam.

We shall develop a simplified model for the dynamics of the absorbing medium which parallels Hänsch and Toschek's treatment of the vapor case.[8]

Section II will describe this polarization spectroscopy technique in more detail and outline the relevant solution of the equations of motion for the density matrix of an inhomogeneously broadened two-level system. Section III will describe the details of our experimental technique and Sec. IV will give the initial results obtained on absorbing organic dyes in liquid solution.

II. THEORY

The simplest energy-level scheme which realistically approximates the dynamics of organic dye systems is diagrammed in Fig. 2.[9] At thermal equilibrium, low-lying vibronic levels within the ground-state manifold are populated. These levels are labeled $|a\rangle$. The incident radiation couples these levels to sublevels of the first excited singlet manifold labeled $|b\rangle$ in Fig. 2. The excited level can decay directly back to level $|a\rangle$ at rate γ_a, or it can decay into a manifold of reservoir states at rate γ_b. The total decay rate of the excited state is then $\Gamma_b = \gamma_b + \gamma_a$. The reservoir state—which can be thought of either as the lowest triplet level or as a vibronically excited level of the ground electronic state—does not interact with the laser fields. Molecules in the reservoir state decay back to the $|a\rangle$ levels at rate Γ_a. The total population of states $|a\rangle$, $|b\rangle$ and the reservoir is assumed constant. We introduce a transverse decay rate Γ_2 ($\Gamma_2 > \Gamma_b$, Γ_a, or $|\Gamma_D|$) which describes the dephasing of coherent superpositions of levels $|a\rangle$ and $|b\rangle$, where $\Gamma_D = \Gamma_a - \gamma_a$.

Such a model neglects several potentially interesting phenomena. In particular, cross relaxation among levels coupled by the radiation field is included only as a dephasing process. The related phenomenon of spectral diffusion is ignored as are the effects of reorientation of the anisotropic absorbing species in a liquid environment.[10-12] Selection rules are also assumed to prohibit transitions between states having the same energy. With these assumptions, it becomes possible to model the absorbing species as an ensemble of two-level systems with a distribution of resonant frequencies ω_0. Such a model, though incomplete, is adequate to describe many of the phenomena observed and to permit the extraction of certain relaxation parameters from the experimental data.

The equations of motion for the elements of the density operator describing the absorbing species

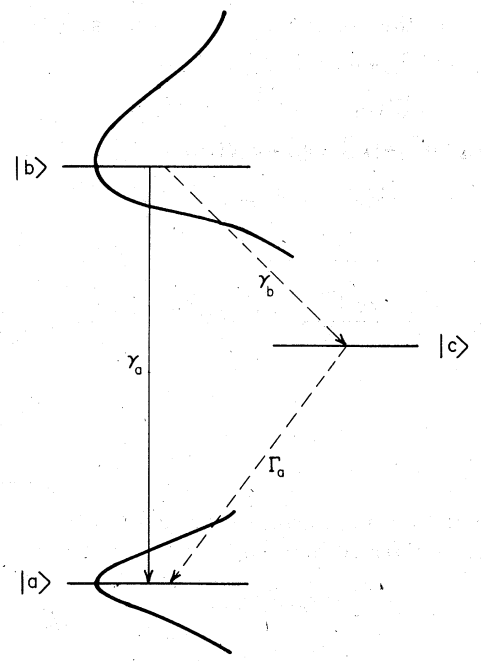

FIG. 2. Energy-level scheme considered in our theory. Real transitions are made from ground level $|a\rangle$ to the excited state $|b\rangle$. The phenomenological reservoir state is represented as $|c\rangle$. γ_a, γ_b, and Γ_a designate population decay rates.

are then

$$\dot{\rho}_{aa} = (-i/\hbar)(H_{ab}\rho_{ba} - \rho_{ab}H_{ba}) + \Gamma_D \rho_{bb} + \Gamma_a(\rho^e - \rho_{aa}), \quad (1)$$

$$\dot{\rho}_{bb} = (i/\hbar)(H_{ab}\rho_{ba} - \rho_{ab}H_{ba}) - \Gamma_b \rho_{bb}, \quad (2)$$

$$\dot{\rho}_{ba} = (i/\hbar)H_{ba}(\rho_{aa} - \rho_{bb}) - (\Gamma_2 + i\omega_0)\rho_{ba}, \quad (3)$$

where the interaction Hamiltonian has nonvanishing matrix elements

$$H_{ba} = H^*_{ab} = -\vec{\mu}_{ba} \cdot (\vec{E}_1 e^{-i\omega_1 t} + \vec{E}^*_1 e^{i\omega_1 t} + \vec{E}_2 e^{-i\omega_2 t} + \vec{E}^*_2 e^{i\omega_2 t}). \quad (4)$$

ρ^e is the equilibrium population of level $|a\rangle$, and the level $|b\rangle$ is assumed unpopulated at equilibrium. The total dielectric polarization is given by

$$\vec{P} = N \int_{-\infty}^{\infty} g(\omega_0) \langle \vec{\mu}_{ab}\rho_{ba} + \vec{\mu}_{ba}\rho_{ab} \rangle \, d\omega_0, \quad (5)$$

where $g(\omega_0)$ is distribution of resonant frequencies describing the total absorption band, N is the density of the absorbing species, and the bracket represents an orientational average over the ensemble.

The steady-state solutions of this set of equations can be written as a sum of Fourier components with amplitudes proportional to ascending

powers of the electric field amplitudes:

$$\rho_{jj} = \rho^e \delta_{ja} + \rho_{jj}^{(2)}(0) + \rho_{jj}^{(2)}(\omega_1 - \omega_2)\, e^{-i(\omega_1-\omega_2)t} + \rho_{jj}^{(2)}(\omega_1 - \omega_2)\, e^{i(\omega_1-\omega_2)t} + \cdots, \tag{6}$$

$$\rho_{ab} = \rho^*_{ba} = [\rho_{ab}^{(1)}(\omega_1) + \rho_{ab}^{(3)}(\omega_1) + \cdots]\, e^{-i\omega_1 t} + [\rho_{ab}^{(1)}(\omega_2) + \rho_{ab}^{(3)}(\omega_2) + \cdots]\, e^{-i\omega_2 t} + \cdots. \tag{7}$$

These amplitudes can be calculated from Eqs. (1)–(3) by the technique of successive approximation. The term in Eq. (7) of interest for polarization spectroscopy oscillates at frequency ω_2 and is bilinear in the amplitude of the field at ω_1. The terms fulfilling this condition and having resonant denominators can be grouped together as

$$\rho_{ab}^{(3)}(\omega_2) = \frac{i\rho^e |\vec{\mu}_{ab}\cdot\vec{E}_1|^2 \vec{\mu}_{ab}\cdot\vec{E}_2}{\Gamma_2 + i(\omega_0 - \omega_2)} \left[\left(\frac{\Gamma_D + \Gamma_b + \Gamma_a}{\Gamma_a \Gamma_b} \right) \left(\frac{1}{\Gamma_2 - i(\omega_0 - \omega_1)} + \frac{1}{\Gamma_2 + i(\omega_0 - \omega_1)} \right) + \left(\frac{1}{\Gamma_a + i(\omega_1 - \omega_2)} + \frac{1}{\Gamma_b + i(\omega_1 - \omega_2)} + \frac{\Gamma_D}{[\Gamma_a + i(\omega_1 - \omega_2)][\Gamma_b + i(\omega_1 - \omega_2)]} \right) \times \left(\frac{1}{\Gamma_2 - i(\omega_0 - \omega_1)} + \frac{1}{\Gamma_2 + i(\omega_0 - \omega_2)} \right) \right], \tag{8}$$

while other nonresonant terms make only slowly varying complex contributions. The intregal in Eq. (5) can be performed to yield the third-order resonant nonlinear polarization vector, as follows:

$$\vec{P}^{(3)}(\omega_2) = \left\langle \frac{2\pi N \vec{\mu}_{ab}\, \rho^e |\vec{\mu}_{ab}\cdot\vec{E}_1|^2 \vec{\mu}_{ab}\cdot\vec{E}_2}{2\Gamma_2 - i(\omega_2 - \omega_1)} \right\rangle g(\omega_0) \left(\frac{\Gamma_D + \Gamma_b + \Gamma_a}{\Gamma_b \Gamma_a} + \frac{1}{\Gamma_a - i(\omega_2 - \omega_1)} + \frac{1}{\Gamma_b - i(\omega_2 - \omega_1)} + \frac{\Gamma_D}{[\Gamma_a - i(\omega_2 - \omega_1)][\Gamma_b - i(\omega_2 - \omega_1)]} \right) \tag{9}$$

where the width of the distribution $g(\omega_0)$ is assumed much larger than Γ_a, Γ_b, and Γ_2. It is convenient to express this result in terms of a third order nonlinear susceptibility tensor

$$P_i^{(3)}(\omega_2) = \sum_{j,k,l} \chi_{ijkl}^{(3)}(-\omega_2, \omega_1, -\omega_1, \omega_2) E_j(\omega_1) \times E_k^*(\omega_1) E_l(\omega_2), \tag{10}$$

where the subscripts now refer to Cartesian coordinates, and by convention the pairing of coordinate and frequency is respected.[13,14] Only two elements of the $\chi^{(3)}$ tensor are necessary to describe the polarization spectroscopy phenomena

$$\chi_{1212}^{(3)}(-\omega_2, \omega_1, -\omega_1, \omega_2) = 2\pi N \rho^e \langle \mu_{x_{ab}} \mu_{y_{ba}} \mu_{x_{ab}} \mu_{y_{ba}} \rangle f(\Delta), \tag{11}$$

$$\chi_{1122}^{(3)}(-\omega_2, \omega_1, -\omega_1, \omega_2) = 2\pi N \rho^e \langle \mu_{x_{ab}} \mu_{x_{ba}} \mu_{y_{ab}} \mu_{y_{ba}} \rangle f(\Delta). \tag{12}$$

In Eqs. (11) and (12), $\Delta = \omega_1 - \omega_2$ is the frequency difference between the two lasers and

$$f(\Delta) = [2\Gamma_2 + i\Delta]^{-1} \left(\frac{\Gamma_D + \Gamma_b + \Gamma_a}{\Gamma_b \Gamma_a} + \frac{1}{\Gamma_a + i\Delta} + \frac{1}{\Gamma_b + i\Delta} + \frac{\Gamma_D}{(\Gamma_a + i\Delta)(\Gamma_b + i\Delta)} \right) \tag{13}$$

is a line-shape function common to all tensor elements in the absence of reorientation. Again the brackets refer to an average over the initially isotropic orientational distribution.

The line-shape function in Eq. (13) is quite general, describing a two-level system unconnected to nonabsorbing reservoir states when $-\Gamma_D = \gamma_a = \gamma_b$ as well as a two-level system relaxing only through a reservoir when $\Gamma_D = \Gamma_a$. The lifetimes of the upper and lower levels are completely unconstrained. In the systems reported here, the various relaxation rates appear to fulfill the inequalities $\Gamma_2 \gg \Gamma_b > \Gamma_a \approx |\Gamma_D|$. The first term in braces in Eq. (13) represents the effect of a steady-state change in the difference of populations of levels $|a\rangle$ and $|b\rangle$. This saturation term is the one exploited in the Doppler-free techniques of polarization spectroscopy. It yields a Lorentzian peak of width $2\Gamma_2$ (HWHM) in a plot of $\mathrm{Im}P^{(3)}(\omega_2)$ as a function of Δ. The remaining terms within the braces result from oscillation of the population difference at frequency Δ. If $\Gamma_2 \gg \Gamma_a, \Gamma_b$ the second and third terms contribute generally Lorentzian peaks with widths equal to the longitudinal relaxation rates of the upper and lower state. Since the area of these two peaks are equal, the narrower will be more prominent in the spectrum. Figure 3 is a series of plots of $|f(\Delta)|^2$ [which is the quantity directly measured in this experiment; see Eq. (13)] for various values of Γ_2/Γ_a and Γ_b/Γ_c. Plots such as these are fit to our experimental data in order to extract relaxation rates. Generally only the fastest (i.e., Γ_2) and slowest (i.e., Γ_a) rates can be at all determined, the

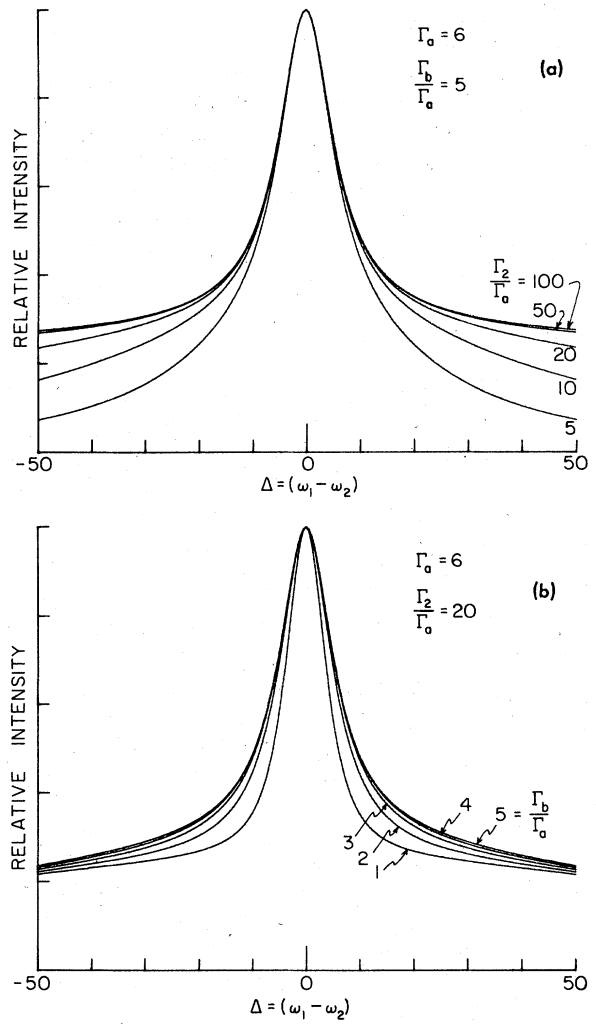

FIG. 3. Computer plot of $|P^{(3)}|^2$. Only the energy denominators are considered (see Eq. 13). (a) Γ_a and Γ_b are fixed and Γ_2 is considered as a parameter. Note that the central-peak feature is insensitive to the changes in Γ_2. (b) Γ_b is varying while Γ_a and Γ_2 are fixed. The central-peak line shape is slightly modified with various values of Γ_b. Since we are considering cases for $\Gamma_b > \Gamma_a$, the curve for $\Gamma_b/\Gamma_a = 1$ represent the case of the largest change in half width.

others presented only as fine details of the line-shape function. Yajima's Rayleigh resonance technique is sensitive only to the three latter terms in Eq. (13). To estimate Γ_2 he must fit fine details in the wings of his lines.[6]

The anisotropic effects detected in this technique also decay as the result of orientational diffusion. For molecules as large as malachite green and cryptocyanine, the orientational diffusion rate is known to be much slower than the electronic decay rates here measured.[15] The effects of reorientation must, however, be considered when longer lifetimes or smaller molecules are studied.

When a linearly polarized probe at ω_2 is used and an elliptically polarized pump at ω_1 with major axis at 45° to the probe polarization plane, the dielectric polarization at ω_2 in the plane orthogonal to the probe is

$$P^{(3)}(\omega_2) \propto (\chi^{(3)}_{1212} + \chi^{(3)}_{1122}) \cos^2 2\phi + i(\chi^{(3)}_{1212} - \chi^{(3)}_{1122}) \sin 2\phi , \quad (14)$$

where $\phi = \arctan (E_{\text{minor axis}}/E_{\text{major axis}})$ defines the ellipticity of the pump wave.[16] For $\phi = 0$ the pump is linearly polarized, while $\phi = \pm 45°$ it is circularly polarized. Then the signal intensity, when normalized to the linear case, can be expressed as

$$I(\omega_2) \propto \cos^4 2\phi + (K_1^2 + K_2^2) \sin^2 2\phi - 2K_2 \sin 2\phi \cos^2 2\phi , \quad (15)$$

where K_1 and K_2 are the real and imaginary part of $(\chi_{1212} - \chi_{1122})/(\chi_{1212} + \chi_{1122})$, respectively. By comparing the intensities as a function of pump ellipticity, one can determine the ratio of the two nonlinear susceptibility tensor elements.

The transparent host material in which the absorbing species is dissolved also has a third-order nonlinear susceptibility. In the case of a liquid composed of nonspherical molecules, this nonlinearity itself should show dispersion with complicated peaks near $\Delta = 0$.[17] Fortunately, the resonant effects in the solute molecules overwhelm the solvent nonlinearities at quite low concentrations.

In order to calculate the intensity radiated as a result of the nonlinear interaction, it is necessary to integrate the wave equation for the detected polarization component in the slowly varying amplitude approximation. A calculation of this sort taking into account the intensity-dependent attenuation of the incident beams is quite laborious; however, a major simplification occurs if it is assumed that the transmission of these intense beams are only slightly different from the low intensity limit. This is equivalent to assuming that the peak intensity produced by the nonlinear interaction is much less than the transmitted probe, a condition well fulfilled in our experiments.

If the pump and probe beams are counterpropagating along the z axis and if the absorbing sample fills the region from $z = 0$ to $z = a$ the equation for the amplitude of the nonlinearly generated polarization component is

$$\frac{\partial E_\perp}{\partial Z} = \frac{4\pi\omega_2}{in_2 c} \chi^{(3)} |E_1(z=a)|^2 E_2(z=0) \times e^{(\beta - 2\beta_2)z - (\beta - \beta_2)a} - \beta_2 E_\perp , \quad (16)$$

where n_2 is the linear index of refraction at ω_2 and

$$\beta_2 = -\frac{1}{E_2}\frac{\partial E_2}{\partial z}, \quad \beta = 2\frac{1}{E_1}\frac{\partial E_1}{\partial z} + \beta_2 .$$

With the boundary condition $E_\perp(z=0)=0$, we obtain

$$E_\perp(z=a) \propto \frac{4\pi\omega}{in_2 c(\beta-\beta_2)}(e^{-\beta_2 a} - e^{-\beta a}) .$$

Clearly the maximum intensity is obtained when

$$a = [1/(\beta_2-\beta)]\ln(\beta_2/\beta)$$

which implies an optimum optical density of 0.48 for the sample if $\beta = 3\beta_2$. In practice it is convenient to work with samples which transmit somewhat more than the optimum amount calculated in this way.

III. EXPERIMENTAL DETAILS

The experimental apparatus used in this work is essentially the same as the one used in our previous work on Raman-induced Kerr-effect spectroscopy and related experiments.[18] Our present setup, which has been modified for this work, is shown in Fig. 1. Two dye laser beams with 8-nsec duration were overlapped temporally and spatially inside the sample cell using 20-cm focal-length lenses and properly situated mirrors. Two dye lasers were simultaneously pumped by the Molectron UV1000 N_2 laser at the repetition rate of 15 Hz. The typical peak pump laser power was 10–30 kW depending on the particular laser dyes used. The linearly polarized, weaker probe beam goes through the crossed polarizer after the sample and analyzed with the Spex 1401 double monochromator and a photomultiplier in conjunction with a Molectron LP 20 boxcar.

The pump beam was most of the time linearly polarized with 45° angle to the probe beam. When needed, $\frac{1}{4}\lambda$ plate was utilized to alter its polarization. The probe and pump wavelengths were chosen to lie within the absorption peak of the investigated dye solution, while ω_1 was changed by turning the grating of the pump laser over the region centered around ω_2.

The counter-propagating geometry of the two beams were chosen to avoid the unwanted stray light from the pump beam going through the spectrometer. This made it possible to scan continuously through the $\omega_1 = \omega_2$ resonance condition. This was the single most essential change from the previous RIKES setup, where two beams with significant frequency difference were propagating in the same direction and minor spatial filtering and use of spectrometer are sufficient to eliminate the pump beam.

The sample cells were 1–2-mm thick and had thin glass windows (0.15-mm thick) to reduce the effects of birefringence. The pump laser power was monitored and recorded in the chart paper simultaneously with the signals. We also recorded the pump laser transmittance through the very samples we used in the polarization spectroscopy experiment. Therefore, any experimental artifacts arising during the frequency scan could be easily discovered and eliminated.

Whenever the dye laser cavity was realigned (e.g., to alter the wavelength radically) the grating positions in the laser cavity were calibrated with respect to absolute wavelength, using the Spex 1401 monochromator. At the same time we carefully examined the laser line shapes at different wavelengths. The half widths (HWHM) of the dye laser beams were found to be 0.4–0.5 cm^{-1} depending on the dyes. With an intracavity etalon, the probe beam half width could be reduced to 0.03 cm^{-1} (HWHM). Typical scanning speed of the pump laser grating was about 0.1 cm^{-1}/sec.

In contrast to our experience with three wave mixing, the polarization spectroscopy signal was very easily found with any sample concentration and the cell length. Once optics were adjusted for best signal level, the only moving part during a run was the pump laser grating.

The measurements were made at room temperature on the organic dyes: malachite green, malachite green oxalate (obtained from Eastman Kodak Co.), and 1, 3′-diethyl-2, 2′ quinolylthiacarbocyanine iodide (Koch-Light Laboratories, U.K.) dissolved in water or ethanol, and an iodine in C_6H_6.

These samples have absorption bands near common dye laser wavelengths and exhibit negligible absorption in the uv at twice the one-photon absorption region. Most of them are known to have relaxation time constants too short to be easily measured using coherent optical transients.

Care was taken in preparing and handling the samples, and an absorption spectrum of each solution was measured to check any impurities. We tried to use freshly mixed samples in each experiment and the solutions were kept at reduced temperatures if storage was necessary. This precaution was employed because we found that temperature and light play a role in discoloring the samples when we kept identical solutions (particularly malachite green solutions) under various conditions over a long (one week) period of time.

IV. RESULTS

In all the samples studied, the experimental traces show a distinct peak centered at $\omega_1 - \omega_2 = 0$

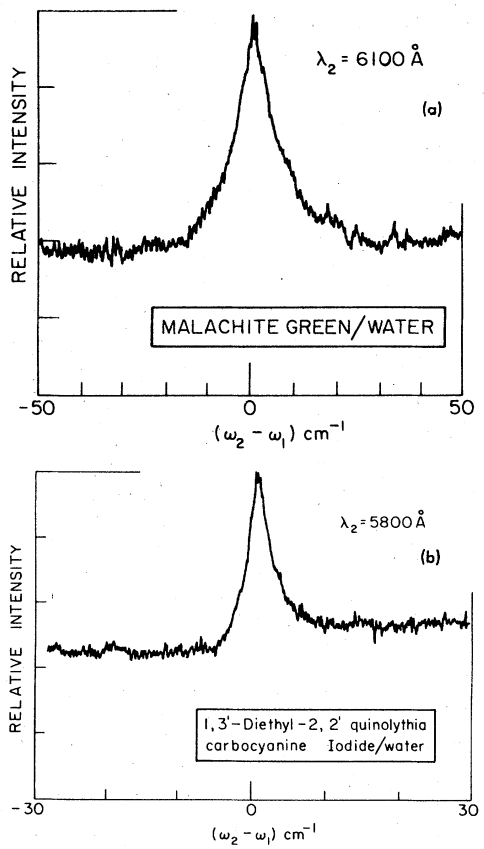

FIG. 4. Experimental traces of the two dye samples. The laser wavelengths are near the center of the absorption peak of each solution. Note the horizontal scale difference between (a) and (b).

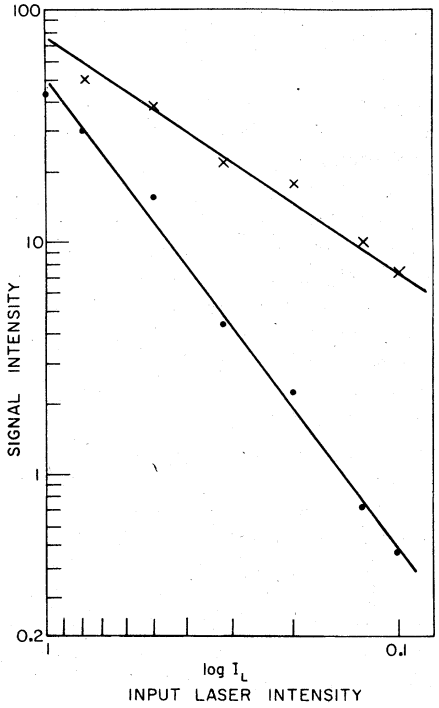

FIG. 5. Dependence of signal intensity on input laser intensities is shown in log-log scale. Experimental points for probe and pump beam are represented by X pulses and solid circles, respectively. The theoretical linear and square law dependences on probe and pump intensity are shown with solid lines.

on top of enhanced background signals. As in Sec. II, ω_1 and ω_2 refer to pump and probe beam frequency, respectively. The signal line shapes are mostly symmetric with respect to zero-frequency difference between ω_1 and ω_2, and the signal reaches the maximum value at $\omega_1 = \omega_2$. In general the line shapes are similar in most of the samples with only the half width of the central peak varying with the absorbing species. For instance, malachite green dissolved in water exhibits a peak of half width, 11 cm^{-1} (FWHM), while only a 3-cm^{-1}-wide peak is observed in cyanine dye solution dissolved in water. The typical traces are shown in Fig. 4. Detailed comparison with theory on the line shape will be discussed later, but several general observations deserve mentioning first.

The signal levels from the absorbing molecules were extremely high and the effects of linear birefringence from the imperfections in optics was negligible in comparison. This is in contrast to the case of RIKES in transparent samples in which birefringence can notably distort line shapes. The possibility that our detected signal was stimulated emission or fluorescence can be excluded by the fact that the signals clearly disappeared when either pump or probe beam was blocked. We have also measured the input laser power dependence of the signal in cyanine dyes and in malachite green solution both at the peak ($\omega_1 - \omega_2 = 0$) and away from the peak ($\omega_1 - \omega_2 \sim 30$ cm^{-1}). We have found that our signals depended linearly on probe laser intensity and quadratrically on the pump intensity over a range of 100 to 1. The results are shown in Fig. 5 for the cyanine dye solution. These measurements are a good indication of the fact that our signals do arise from $\chi^{(3)}$ and higher-order effects or saturation of the nonlinearity need not be considered in our data analysis.

The contributions to the detected signal from the solvent in which the dye molecules are dissolved, should be also considered. To find its particular characteristics, the nonlinear signal was separately measured with each pure solvent and the line shapes were compared to those of the solution. We found that the solvent contributions not only had different linewidths and peak to background ratio, but these signals were two

to six orders of magnitude smaller than those from the dye solutions. Thus, any interferences or complications due to the solvent signals, can be excluded from our analysis. It is worthwhile to note that the solvent signals are not resonantly enhanced through one-photon absorption and will decrease as the concentration of the absorbing species is increased.

We also experimentally investigated the line shapes of the signal as the polarization of the pump beam was changed by use of $\frac{1}{4}\lambda$ plate. As predicted in Sec. II, essentially the same line shapes were observed regardless of the ellipticity of the pump beam. Only the signal level decreased by a factor of 30–50 as the pump beam changed from the linear to circular polarization. By carefully measuring this polarization dependence of the signal we were able to deduce the relative value of the two tensor elements of $\chi^{(3)}$ which influence our signal. From Eq. (14) in Sec. II, we can see that $I(\omega_2) \propto |\chi_{1212} - \chi_{1122}|^2$ for circular pump and that the signal will be zero if $\chi_{1212} = \chi_{1122}$. In Fig. 6 the signal level for malachite green in water normalized to the linear case is plotted as a function of ϕ, which specifies the ellipticity of the pump beam. The solid line is the calculated curve using Eq. (15) and with K_1 and K_2 values as 0.14 and 0.03, respectively. Similar values were deduced for other samples also. This observation is evidence that the Kleinman symmetry holds approximately even in the one-photon resonance region.[19]

Experimental traces were analyzed using the formula given in Eq. (13) of Sec. II. Each data trace was visually fit to the computer generated plot with the assumption that $\Gamma_2 \gg \Gamma_b, \Gamma_a$. The central peak is rather insensitive to the Γ_2 values and reflects the longitudinal relaxation rates

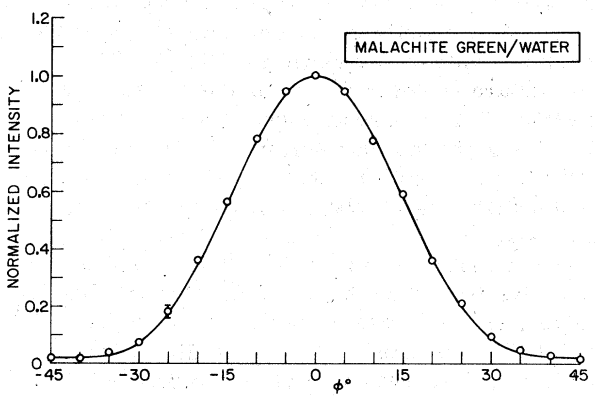

FIG. 6. Signal intensity vs the pump beam ellipticity. The circles are experimental points and a typical error bracket is affixed to one point. The solid line represents the theoretical curve obtained from Eq. (15).

(Γ_a, Γ_b) only. In fitting our data, we further assumed that $\Gamma_b > \Gamma_a \approx \Gamma_D$, which means that excited molecules relax mostly through radiationless process and that the relaxation rate from state $|b\rangle$ to the reservoir state is faster than that from the latter to the ground level $|a\rangle$. Then the half width of the central peak is the measure of Γ_a, the ground-state recovery time and other parameters only minutely modify the line shape. Considering the fact that the central peak half width is much larger than the laser half width, convolution with the laser linewidth was not carried out.

With $\Gamma_2/\Gamma_a \geq 20$, we deduced $1/\Gamma_a$ to be 1.2 ± 0.1 psec for malachite green dissolved in water and 3.4 ± 0.4 psec for the cyanine dye in the same solvent, with incident laser wavelengths at 6100 and 5800 Å, respectively. These wavelengths almost coincide with the center of the absorption peak of each solution. We also observed that malachite green and malachite green oxalate exhibit the same central-peak half width. It is interesting to note that had we used the assumption $\Gamma_b \approx \Gamma_a$, instead of $\Gamma_b > \Gamma_a$, $1/\Gamma_a$ of malachite green is deduced to be 0.9 psec; only 25% different from 1.2 psec deduced above. This indicates that as long as the ground-state recovery time ($1/\Gamma_a$) is longer than the upper state ($|b\rangle$) depopulation rate ($1/\Gamma_b$), our data definitely provides a lower limit of $1/\Gamma_a = 0.9$ psec and an upper limit of 1.2 psec.

Equation (9) shows a high degree of symmetry between the rates Γ_a and Γ_b. The arguments of the previous paragraph also apply to the case $\Gamma_b < \Gamma_a$ in which the equilibrium population of the lower level recovers more rapidly than the upper level decays. This case can occur theoretically when the reservoir state is thermally populated, but is not thought to be common. While there thus can be some ambiguity in the interpretation of the width of the central peak of the polarization spectroscopy spectrum without prior knowledge of the relative magnitudes of Γ_a and Γ_b, that width does represent the slowest population decay rate in the $|a\rangle - |b\rangle$ level system.

Two different measurements of relaxation rate in malachite green in methanol or ethanol were recently reported.[5,20] Both techniques involve ultrashort (psec) laser pulses and the measurements were carried out in time domain. Ippen and Shank have measured the absorption recovery time at $\lambda = 6150$ Å to be 2.1 psec, but they considered this as the ground-state repopulation time and predicted a much shorter excited state ($|S_1\rangle$) lifetime based on the quantum yield measurement of Forster *et al.*[21] Their theoretical model is directly compared to ours if we set $\Gamma_D \gg \Gamma_a$. In this case, our value of ground-state recovery

time (1.2 psec) is in reasonable agreement with theirs. Another, but more recent, measurement by Wirth *et al.* utilizes different techniques: two-photon fluorescence measurement.[20] By observing the fluorescence from $|S_2\rangle$ level after consecutive two-photon absorption, they deduce the $|S_1\rangle$ lifetime as 5 ± 3 psec. ($|S_1\rangle$ and $|S_2\rangle$ are first and second excited electronic state, respectively.) This value is quite a lot larger than Ippen and Shank's prediction of the $|S_1\rangle$ state lifetime, and also differs from ours even if we assume that $\Gamma_b \gg \Gamma_a$. However, in view of their experimental difficulties such as the large laser pulse width (13 ± 1 psec) and very weak S_2-fluorescence intensities, their results do not seem to be seriously inconsistent with ours. Unfortunately, to our knowledge no relaxation rate measurement exists on the cyanine dye we studied.

As the laser wavelengths were varied from the center to different points of the absorption peak, we observed that the central-peak half width is somewhat altered. Specifically, the half width of the malachite green at 5800 Å is 24% narrower than that at 6100 Å, but for the cyanine dye, it is about 20% narrower at 6100 Å than that at 5800 Å. If we assume the same theoretical model at all incident wavelengths, our results indicate that the ground-state recovery time is longer at the center of the absorption. We can also speculate that this change arises from neglecting spectral diffusion or cross relaxation mechanisms in our theory. In any case, we do not see an order of magnitude change in this half width as Yajima *et al.* have indirectly deduced from an effective T_1 measurement using a CARS technique.[6]

The polarization spectra of molecular iodine dissolved in benzene were quite different from the spectra obtained in the organic systems. In iodine, the only feature attributable to the absorbing species was a peak centered at $\Delta = 0$ with a shape that reproduced the spectrum of our pump laser. We interpret this observation to mean that all of the lifetimes and the dephasing time $1/\Gamma_2$ in the iodine-benzene system are longer than the 10 psec that represents the longest relaxation time leading to a resolvable linewidth with our laser system. Previous papers have shown that the lower level recovery time of this system is ≈ 1 nsec, and our measurements imply a lower limit on $1/\Gamma_2$ of 10 psec.[22]

The theory presented in Sec. II implies that broad structure observed in the spectra of the organic dyes should have a width $2\Gamma_2$. This feature of the spectrum arises simply from the intensity dependent dichroism that is produced when the polarized pump laser bleaches one set of molecules and not another. On a frequency scale of a few tens of cm^{-1}, this broad structure appears quite flat, which implies a dephasing time ≤ 0.1 psec for these organic samples.

It is necessary to scan a wider range of Δ in order to obtain a more exact estimate of Γ_2 from the structure of this background feature. The range of frequencies, necessary in such an experiment, exceeds the continuous tuning range of our lasers. We have, however, examined the broad background structure of the cryptocyanine dye dissolved in ethanol using wavelengths $\lambda_2 = 5800$ Å and $6100 < \lambda_1 < 6400$ Å. Thus we were able to scan the range $850 < \Delta < 1600$ cm^{-1}. In this region the nonlinear signal still was dominated by the saturation background of the absorbing species. The polarization spectrum roughly paralleled the absorption spectrum in this region, implying a dephasing time less than 10 fm sec. Similar results were also obtained in malachite green.

Recent data on the time evolution of the absorption of similar systems obtained using picosecond lasers supports our contention that the homogeneous linewidths of transitions in these organic dyes are essentially equal to the width of the absorption spectrum.[23] On the other hand, the line shapes observed and spectral hole-burning experiments have been interpreted to imply a homogeneous linewidth of order 100 fm sec in some other organic dyes.[6,10] Careful fitting of subtle features of the observed lineshape functions were necessary in obtaining these contradictory results, while our estimates of Γ_2 depend only on the presence or absence of a resonantly enhanced signal at a particular value of Δ.

The analysis leading to Eq. (9) assumed that the distribution of resonant frequencies was wider than the homogeneous linewidth of any one transition. If this assumption is invalid, one can expect to find discrepancies between the observed lineshapes and the function in Eq. (13). Such a discrepancy does appear in the ratio of the maximum signal observed at $\Delta = 0$ to the background level due to the component of width $2\Gamma_2$. Equation (13) implies that the ratio of detected intensities should be 4 : 1, since at $\Delta = 0$ the contribution of the first term in braces in Eq. (13) equals the sum of the other three. In fact this ratio varies from 3.2 : 1 for malachite green oxalate in water solution, to less than 2 : 1 for the cyanine dye in high-viscosity solvents. More complex models of the dynamics of density matrix fail to account for this discrepancy. The nonresonant terms neglected in the analysis of Sec. II are not expected to be large enough to cause such a significant change in the peak to background ratio. One must therefore conclude that the simple model presented in Sec. II does not completely describe the dy-

namics of absorbing organic dyes in liquid solution.

V. CONCLUSIONS

We have described a technique of polarization spectroscopy that is useful for elucidating the relaxation rates of transitions in condensed media, and have presented a simple theory which describes the expected phenomena. Significant parts of this theoretical model are confirmed by a series of experiments performed on absorbing species in liquid solution. The discrepancies observed appear related to the complexities of these systems, rather than to any intrinsic limitation of the technique. Relaxation rates have been determined which are consistent with previous measurements and with prior expectation.

The technique proposed may prove most useful in studying relaxation phenomena in crystals and glasses in spectral regions where reliable picosecond lasers do not yet exist. Time-domain measurements in such systems cannot now be conveniently performed, but tunable lasers suitable for polarization spectroscopy now cover the range from 3400 Å to 3 μm. Systems with relaxation times up to several nanoseconds can be studied using single-mode lasers, but the technique is more easily applied to phenomena occurring on the picosecond and subpicosecond time scale. The polarization spectroscopy technique therefore compliments previously developed methods employing coherent transients or other forms of wave mixing.

ACKNOWLEDGMENTS

One of the authors (J. J. S.) would like to thank Professor R. W. Hellwarth for many illuminating discussions. This research was supported in part by the National Science Foundation under Grant Nos. DMR 76-14881 and DMR 77-11326.

[1]N. Bloembergen, M. D. Levenson in *Topics in Applied Physics, High-Resolution Laser Spectroscopy*, edited by K. Shimoda (Springer-Verlag, Berlin, 1976), Vol. 13.
[2]V. S. Letokhov and V. P. Chebotayev, in *Nonlinear Laser Spectroscopy*, edited by D. L. MacAdam, (Springer-Verlag, Berlin, 1977), Vol. 4.
[3]R. G. Brewer, in *Frontiers in Laser Spectroscopy*, edited by R. Balian, S. Haroche, and S. Liberman (North-Holland, Amsterdam, 1977).
[4]A. Szabo, Phys. Rev. Lett. 25, 924 (1970).
[5]E. P. Ippen, C. V. Shank, and A. Bergman, Chem. Phys. Lett. 38, 611 (1976).
[6]T. Yajima, Opt. Commun. 14, 378 (1975); T. Yajima, H. Souma, and Y. Ishida, Phys. Rev. A 17, 324 (1978).
[7]C. Wieman and T. W. Hänsch, Phys. Rev. Lett. 36, 1170 (1976); R. Teets, R. Feinberg, T. W. Hänsch, and A. L. Schawlow, *ibid.* 37, 683 (1976).
[8]T. W. Hänsch and P. Toschek, Z. Phys. 236, 213 (1970).
[9]Bela A. Lengyel, *Lasers*, 2nd ed. (Wiley-Interscience, New York, 1971), Chap. 8.
[10]G. Mourou, IEEE J. Quant. Elec. 11, 1 (1975).
[11]H. E. Lessing, A. VonJena, Chem. Phys. Lett. 42, 213 (1976).
[12]P. M. Selzer, D. S. Hamilton, and W. M. Yen, Phys. Rev. Lett. 38, 858 (1976).
[13]R. W. Hellwarth, in *Progress in Quantum Electronics* edited by J. H. Sanders and S. Stenholm (Pergamon, Oxford, England, 1977), Vol. 5, No. 1.
[14]M. D. Levenson and N. Bloembergen, Phys. Rev. B 10, 4447 (1974).
[15]C. V. Shank and E. P. Ippen, Appl. Phys. Lett. 26, 62 (1975).
[16]M. D. Levenson and J. J. Song, J. Opt. Soc. Am. 66, 641 (1976).
[17]H. E. Howard-Lock and R. S. Taylor, Can. J. Phys. 52, 2436 (1974).
[18]J. J. Song and M. D. Levenson, J. Appl. Phys. 48, 3496 (1977).
[19]D. A. Kleinman, Phys. Rev. 126, 1977 (1962).
[20]P. Wirth, S. Schneider, and F. Dörr, Opt. Comm. 20, 155 (1977).
[21]Th. Förster and G. Hoffmann, Z. Phys. Chem. 75, 63 (1971).
[22]Kenneth B. Eisenthal, in *Laser Spectroscopy*, edited by S. Haroche, J. C. Pebay-Peyroula, T. W. Hänsch, and S. E. Harris (Springer-Verlag, Berlin, 1975), p. 390.
[23]C. V. Shank and E. P. Ippen (private communication).